



HAL
open science

Preface to the Special Section: Dense Water Formations in the Northwestern Mediterranean: From the Physical Forcings to the Biogeochemical Consequences

Pascal Conan, Pierre Testor, Claude Estournel, Fabrizio d'Ortenzio, Mireille Pujo-Pay, Xavier Durrieu de Madron

► **To cite this version:**

Pascal Conan, Pierre Testor, Claude Estournel, Fabrizio d'Ortenzio, Mireille Pujo-Pay, et al.. Preface to the Special Section: Dense Water Formations in the Northwestern Mediterranean: From the Physical Forcings to the Biogeochemical Consequences. *Journal of Geophysical Research. Oceans*, 2018, 123 (10), pp.6983-6995. <10.1029/2018JC014301>. <hal-02190724>

HAL Id: hal-02190724

<https://hal.science/hal-02190724v1>

Submitted on 15 Feb 2021

HAL is a multi-disciplinary open access archive for the deposit and dissemination of scientific research documents, whether they are published or not. The documents may come from teaching and research institutions in France or abroad, or from public or private research centers.

L'archive ouverte pluridisciplinaire **HAL**, est destinée au dépôt et à la diffusion de documents scientifiques de niveau recherche, publiés ou non, émanant des établissements d'enseignement et de recherche français ou étrangers, des laboratoires publics ou privés.



HAL Authorization

1 Preface to the Special Section: Dense water formations in the North Western
2 Mediterranean: from the physical forcings to the biogeochemical consequences

3
4 Pascal Conan¹, Pierre Testor², Claude Estournel³, Fabrizio D'Ortenzio⁴, Mireille Pujo-Pay¹,
5 Xavier Durrieu de Madron⁵

6
7 ¹ Sorbonne Université, UPMC, Univ. Paris 06, INSU-CNRS, UMR 7621, Laboratoire d'Océanographie
8 Microbienne (LOMIC), Observatoire Océanologique de Banyuls, 66650 Banyuls-sur-Mer, France

9 ² Sorbonne Université, UPMC, Univ. Paris 06, CNRS-IRD-MNHN, Laboratoire d'Océanographie et du
10 Climat : Expérimentation et Approches Numériques (LOCEAN), IPSL, 75252 Paris, France

11 ³ Laboratoire d'Aérodynamique, Université de Toulouse, CNRS, UPS, 14 avenue Edouard Belin, 31400
12 Toulouse, France

13 ⁴ Sorbonne Université, UPMC Univ. Paris 06, INSU-CNRS, UMR 7093, Laboratoire d'Océanographie de
14 Villefranche, 181 Chemin du Lazaret, 06230 Villefranche-sur-Mer, France

15 ⁵ Université de Perpignan Via Domitia, CNRS UMR 5110, Centre d'Etude et de Formation sur les
16 Environnements Méditerranéens, 52 avenue Paul Alduy, 66860 Perpignan, France

17
18 Correspondence to: P. Conan; pascal.conan@obs-banyuls.fr

19
20
21
22 Short Abstract..... 2
23 Key Points 3
24 Program acronyms 3
25 1. Rationales 4
26 2. Strategic plan..... 6
27 3. Major outcomes 8
28 3.1. Dynamics of the atmosphere and air-sea fluxes 8
29 3.2. Interannual variability of dense water formation 9
30 3.3. Deep water formation during winter 2013 10
31 3.4. Effects of small scales and intrinsic ocean variability on dense water formation 11
32 3.5. Effect of dense water formation on biogeochemical budgets and primary production 12
33 3.6. Zooplankton community response to dense water formation 14

36 **Short Abstract**

37 The northwestern Mediterranean Sea is one of the few sites of open-sea deep convection and dense
38 water formation. The area is characterized by intense air-sea exchanges favored by the succession of
39 strong northerly and northwesterly winds during autumn and winter that eventually induce deep
40 convection episodes and the formation of the 'Western Mediterranean Deep Water'. This region
41 exhibits a significant spring phytoplankton bloom, which appears to be largely influenced in intensity
42 and diversity by the winter mixing.

43 To understand and resolve the interplay between the atmosphere and ocean, and the impact of
44 ocean circulation and mixing on biogeochemistry, we carried out an unprecedented observational
45 effort during a large experiment between July 2012 and July 2013. A multiplatform approach -
46 combining aircraft, balloons, ships, moorings, floats, and gliders - aimed both at characterizing the
47 dynamics of the atmosphere and at quantifying the physical, biogeochemical and biological
48 properties of the water masses. Beyond a better understanding of the wind dynamics, the
49 interannual variability of the deep convection, and the seasonal variability of the nutrient distribution
50 and plankton structure in the pelagic ecosystem, the experiment provided a reference data set that
51 was used as a benchmark for advancing the modeling of the surface fluxes, convective processes,
52 dense water formation rates, and physical-biogeochemical coupling processes. It also represented an
53 opportunity for complementary investigations such as evaluating model parameterizations or
54 studying the role of sub-mesoscale eddies in dense water spreading and biogeochemistry.

55

56 **Detailed Abstract**

57 Open sea deep convection and dense water formation constitute an important driving mechanism
58 for the ocean circulation and ventilation. This mechanism also strongly impacts the nutrients
59 distribution and controls the triggering of the blooms of the first producer levels and then, the
60 structure and organization of the whole trophic network. It is particularly sensitive to changes in
61 environmental conditions. It is expected to increase/decrease because of weaker/stronger
62 stratification due to ocean warming and evaporation.

63 The northwestern Mediterranean Sea is one of the few sites of open-sea deep convection and dense
64 water formation. The area is characterized by intense air-sea exchanges favored by the succession of
65 strong northerly and northwesterly winds during autumn and winter that eventually induce deep
66 convection episodes and the formation of the 'Western Mediterranean Deep Water'. This region
67 exhibits a significant spring phytoplankton bloom, which appears to be largely influenced in intensity
68 and diversity by the winter mixing.

69 High-resolution, realistic, three-dimensional atmospheric and oceanic models are essential for
70 assessing the intricacy of buoyancy fluxes, horizontal advection, and convective processes, but they
71 need to be validated by data that describe the variability of convection at small spatial scales (a few
72 kilometers) and at high frequency (typically a day), and by accurate concomitant observations
73 throughout the water column and atmosphere, especially during strong wind events. Likewise, the
74 lack of *in situ* observations simultaneously inferring the main physical and biogeochemical variables
75 was a major obstacle to unify a consensual description of the variability of the phytoplankton spring
76 bloom and finally to equilibrate matter fluxes and budgets over an annual cycle.

77 To understand and resolve the interplay between the atmosphere and ocean, and the impact of
78 ocean circulation and mixing on biogeochemistry, we carried out an unprecedented observational
79 effort during a large experiment between July 2012 and July 2013. A multiplatform approach -
80 combining aircraft, balloons, ships, moorings, floats, and gliders - aimed both at characterizing the

81 dynamics of the atmosphere and at quantifying the physical, biogeochemical and biological
82 properties of the water masses. Beyond a better understanding of the wind dynamics, the
83 interannual variability of the deep convection, and the seasonal variability of the nutrient distribution
84 and plankton structure in the pelagic ecosystem, the experiment provided a reference data set that
85 was used as a benchmark for advancing the modeling of the surface fluxes, convective processes,
86 dense water formation rates, and physical-biogeochemical coupling processes. It also represented an
87 opportunity for complementary investigations such as evaluating model parameterizations or
88 studying the role of sub-mesoscale eddies in dense water spreading and biogeochemistry.

89
90

91 **Key Points**

- 92 • Dynamics of dense water formation and effects of (sub)mesoscale dynamics and intrinsic ocean
93 variability
- 94 • Estimates of dense water formation rate, characteristics, and fate
- 95 • Effect of deep water formation on biogeochemical budgets, planktonic biodiversity and trophic
96 levels functioning
- 97 • Potential evolution of mechanisms and their impacts on biogeochemistry in the context of global
98 change

99

100

101 **Program acronyms**

102	DeWEX:	Deep Water formation Experiment
103	HyMEX:	Hydrological cycle in the Mediterranean EXperiment
104	MERMEX:	Marine Ecosystems Response in the Mediterranean Experiment
105	MISTRALS:	Mediterranean Integrated Studies at Regional And Local Scales
106	MOOSE:	Mediterranean Ocean Observing System on Environment
107	NAOS:	Novel Argo Ocean observing System
108	PERSEUS:	Protection EuROpean Seas and borders through the intelligent Use of surveillance

109

110

111

112

113 1. Rationales

114 The Mediterranean Sea is recognized to be particularly sensitive to climate change [*Adloff et*
115 *al.*, 2015; *Cacho et al.*, 2002; *Giorgi*, 2006; *Somot et al.*, 2006]. The basin is affected by an increasing
116 anthropogenic pressure, linked to strong economical and touristic activities [*i.e. Attané and*
117 *Courbage*, 2001]. Its semi-enclosed nature, together with its smaller inertia [*Paluszkiewicz*, 1994]
118 compared to large oceans [*Lacombe and Richez*, 1982], makes it more sensitive to natural variations
119 in the atmosphere-ocean and land-ocean interactions and exchanges, which can, in turn, enhance
120 the effects of climatic perturbations. The Mediterranean Sea is one of the most intricate marine
121 environments on Earth as most of the critical physical processes characterizing the global circulation
122 (dense water formation, thermohaline circulation, sub-basins gyres...) can be observed in a narrow
123 latitudinal belt at mid-latitudes. They act on a large spectrum of spatial and temporal scales
124 [*MERMEX group*, 2011], and induce a pronounced biological heterogeneity [*Conan et al.*, 1999; *Crise*
125 *et al.*, 1999; *Robinson et al.*, 2001]. It combines a clear West - East gradient in nutrients distribution
126 and oligotrophy [*D'Ortenzio and Ribera d'Alcalà*, 2009; *Pujo-Pay et al.*, 2011; *Ribera d'Alcalà et al.*,
127 2003] with a high spatio-temporal variability in the dynamics of nutrients and organic matter [*Pujo-*
128 *Pay and Conan*, 2003; *Pujo-Pay et al.*, 2011; *Santinelli et al.*, 2010] which is propagated through
129 diverse bottom-up and top-down controls within primary, secondary and upper trophic levels.

130 The Mediterranean Sea can thus be regarded as a reduced model of the global ocean and, in
131 this context, the North Western Mediterranean (NWM hereafter) is consensually assumed as a
132 critical region for the functioning of the whole basin. In this relatively small portion of the
133 Mediterranean Sea, deep convection is regularly observed in winter. If the three phases of
134 convection (preconditioning, vertical mixing and spreading/ restratification) have been defined for
135 several decades [*MEDOC group*, 1970], it appears that these phases overlap and that the physical
136 processes that govern them interact in a wide range of spatial and temporal scales. In particular,
137 small-scale and sub-mesoscale dynamics play a particularly important role, for example convective
138 plumes whose size is less than one kilometer and which are important mixing agents, or sub-
139 mesoscale coherent vortices of radius (~5km) which are involved in the large scale circulation of the
140 newly formed deep water [*Testor and Gascard*, 2003].

141 Convection induces a redistribution of organic and inorganic matters all over the water
142 column. Moreover, in the same area (although with a larger extension and with a greater interannual
143 variability than the region of deep convection) a large and intense spring bloom is observed
144 [*D'Ortenzio and Ribera d'Alcalà*, 2009; *Mayot et al.*, 2016], presenting a high variability from
145 mesoscale to small scale, often clearly coupled to the physical one [*Diaz et al.*, 2000]. The bloom
146 represents the most important process of the basin in terms of primary and secondary productions

147 at the origin of large carbon exports to the deep layers [*MERMEX group*, 2011]. In such areas, the
148 intermittent nutrient enrichment promotes a switching between a small-sized microbial community
149 and diatom-dominated populations [*Conan et al.*, 1999; *Siokou-Frangou et al.*, 2010]. In the Ligurian
150 Sea, for example, *Marty and Chiavérini [2010]* found a strong relationship between the depth of the
151 wintertime convection and nutrient enrichment of the surface layer, triggering short and intense
152 diatom production and deep vertical flux before the onset of the stratification and the development
153 of the regular spring bloom [*Stemmann et al.*, 2002]. Higher abundance of zooplankton in the '80s
154 and late '90s was also correlated with dry and cold winters [*Vandromme et al.*, 2011]. Besides, the
155 modeling results of *Auger et al. [2014]* indicated that the total annual phytoplankton biomass is
156 favored by convection because of the reduced zooplankton grazing pressure in winter and early
157 spring while the annual primary production is not affected due to a compensation of its reduction in
158 winter by its increase in spring.

159 All the above demonstrates that the NWM area concentrates several physical biological and
160 chemical processes that are absolutely critical for the Mediterranean functioning, but that are also
161 dramatically relevant to understand the complex interplay between physical forcing and
162 biogeochemical responses at a synoptic view. However, and despite of several national and
163 international initiatives, the strong imbrications of spatial (from meso- to large-) and temporal (from
164 episodic- to interannual-) scales of the main processes involved limited our comprehension of the
165 functioning of the area and of its role in a Pan-Mediterranean context.

166 In a review paper devoted to the Mediterranean Sea [*MERMEX group*, 2011], the inadequacy
167 of the observational approaches, which were in the past for the most based on punctual cruises or a
168 small number of fixed observing systems (and as such cannot be extrapolated to a wider spatial
169 context or only under very specific hypotheses) was identified as the critical limitation for our
170 understanding of the region. The Deep Water Formation (DWF hereafter) process generally occurs
171 during a period of less than one month, with a low interannual variability in the timing of the deep
172 convection phase [*Houpert et al.*, 2016]. On the other hand, the DWF is pre-conditioned during at
173 least the whole previous fall [*Madec et al.*, 1996] and possibly previous winter periods. Moreover,
174 the impact of the Levantine Intermediate Water (LIW) on the DWF was acknowledged [*Grignon et al.*,
175 2010]. The previous observational approaches were inadequate to completely describe the
176 succession of the DWF phases. For the biological and chemical observations, this inadequacy was
177 even more flagrant, with a consequence that, despite of some fixed stations or satellite monitoring,
178 the seasonality of the biogeochemical dynamic of the area was still missing.

179 A large experiment coupling the exploration of the ocean from the physical and biological
180 point of views to observations of the air-sea interface and atmospheric boundary layer was then

181 designed to couple the recent technological breakthroughs for small and intelligent autonomous
182 platforms with satellite remote sensing (altimetry, SST, and color) information, with more 'classical'
183 data acquisition by ship and aircraft sampling, and with existing fixed point moorings. The number of
184 oceanic observations was dramatically high compared to previous experiments, and, more
185 importantly, observations were obtained all along a seasonal cycle. These data were directly used in
186 combination with models, before, during and after the observational phase. The strategy was
187 focused on:

- 188 • the understanding, in a wide range of spatial and temporal scales of the physical mechanisms
189 and forcing that precondition the convection zone, form dense water and disperse it
- 190 • the role of deep winter convection on the biogeochemical properties of the water masses, on
191 the resulting organization of the pelagic ecosystems in spring and on the organic matter export

192 The modeling activity was central for driving the sampling strategy before the observation phase, for
193 integrating the observations in a complete 4D frame during the observation phase, while favoring
194 the understanding of the integrated system and improving our long-term simulations and scenarii.
195 All these efforts allowed us to obtain a unique and comprehensive data set to validate and improve
196 the physical/ biogeochemical coupled models.

197 The objective of this special issue is to synthesize the major results of these experiments and
198 related operations. These results bring significant advances in our understanding of the dynamics of
199 DWF and the related functioning of marine ecosystems that have been organized according to six
200 major axes:

- 201 ● Dynamics of the atmosphere and air-sea fluxes
- 202 ● Interannual variability of dense water formation
- 203 ● Deep water formation during winter 2013
- 204 ● Effects of small scales and intrinsic ocean variability on dense water formation
- 205 ● Effect of deep water formation on biogeochemical budgets and primary production
- 206 ● Response of zooplankton community to dense water formation

207

208

209 **2. Strategic plan**

210 The experimental strategy was based on pooling the DeWEX [Testor *et al.*, 2018] and HyMeX
211 SOP2 [Estournel *et al.*, 2016b] projects respectively supported by the MerMEX and HyMEX programs
212 (both components of MISTRALS). Several National and European projects (i.e. RemOCEAN ERC, NAOS
213 EquipEx, FP7-GROOM, FP7-JERICO, FP7-PERSEUS), combined with the long lasting monitoring activity

214 of MOOSE and with some additional surveys (*i.e.* MerMEX WP2-SPECIMED), provided a solid and
215 favorable context contributing to the success of this experiment.

216 The observational strategy was mainly driven by the need to obtain pertinent observations
217 all along a seasonal cycle. Six cruises were then programmed at key moments of the year 2012-2013
218 (see figure 1). This intensive ship-based observation effort, carried out from July 2012 to September
219 2013, was completed by a large variety of tools, for the most robotic or semi-robotic, to obtain a
220 quasi-synoptic view of the area, to interpolate between the cruises and to provide enough
221 observations to initialize models (Fig. 1).

222 The observation strategies involved then several airborne (aircraft and atmospheric
223 boundary layer balloons), surface (boat, fixed and drifting buoys), and oceanic (physical and bio-
224 optical Argo floats and gliders, mooring lines equipped with CTD sensors, current-meters and
225 sediment traps) platforms (Fig. 2 and 3). Space observations of the sea surface altimetry and ocean
226 color were used to monitor the interannual variability and spatial extent of the convection. The ATR-
227 42 aircraft operated by the "Service des Avions Français Instrumentés pour la Recherche en
228 Environnement (SAFIRE)", investigated the mean and turbulent characteristics of the marine
229 atmospheric boundary layer above the oceanic convection region. Boundary layer pressurized
230 balloons, developed by the "Centre National d'Etudes Spatiales", were used to document the
231 evolution of the thermo-dynamical characteristics along the trajectory of air parcels during northern
232 wind (Mistral) events.

233 Measurements from research vessels (R/V L'Atalante, R/V Le Suroît, and R/V Tethys II) were
234 intended to be operated over periods of 3 weeks in order to cover most of the NWM during different
235 key phases of the seasonal cycle of the region. The six cruises were carried out in July-August 2012
236 (summer stratified period), September 2012 (summer-to-fall transition stratified period), February
237 2013 (pre-bloom, winter mixing period), April 2013 (spring bloom, restratification and spreading
238 period), July 2013 (post bloom and restratified period) and September 2013. The February DeWEX
239 2013 cruise, which took place during the period of intense mixing, overlapped with the airborne
240 observations. Only during naval operations, a very large set of chemical and biological data were
241 collected, in particular to provide stocks, fluxes, diversities and biological activities. During all the
242 cruises, a CTD carousel composed of 12 Niskin bottles was deployed and discrete samples were
243 collected. 440 surface-to-bottom profiles of CTD and of biogeochemical parameters (chlorophyll-a,
244 dissolved oxygen, turbidity, currents, aggregates and zooplankton images), 9240 water samples for
245 nutrients, dissolved and particulate organic matter, pigments, microbial diversity were collected.
246 During February and April 2013 cruises, primary and bacterial productions were measured, and
247 additional vertical net hauls were performed to collect zooplankton.

248 Surface and ship-based observations were also collected over the whole NWM. Numerous profiles
249 in the upper layer between the surface and 1000 or 2000 m deep were collected with Argo and BGC-
250 Argo profiling floats and gliders. All these platforms were equipped with CTD sensors, and some
251 platforms also carried biogeochemical sensors (i.e. chlorophyll-a, dissolved oxygen, nitrate, optical
252 backscattering). After interoperability processes, the moorings, profiling floats, and gliders provided
253 an opportunity to characterize the temporal variability of the oceanic conditions throughout the
254 year, and small-scale features, such as sub-mesoscale eddies and convective plumes. Surface drifters
255 (SVP and Marisonde buoys) and fixed meteorological buoys ("Lion" and "Azur Météo-France" buoys)
256 were used to collect air-sea interface parameters. Long mooring lines in the convection region
257 ("Lion") and in the Ligurian Sea ("Dyfamed") provided additional observations of the evolution of the
258 mixed layer depth, water masses, currents, and particle fluxes.

259

260 **3. Major outcomes**

261 **3.1. Dynamics of the atmosphere and air-sea fluxes**

262 The winter-integrated buoyancy loss over the Gulf of Lion was identified as the primary
263 driving factor of the DWF interannual variability [*Somot et al., 2016*]. At a daily scale, the Atlantic
264 Ridge weather regime was identified as favorable to the Mistral wind and associated strong
265 buoyancy losses and therefore to DWF, whereas the positive phase of the North Atlantic Oscillation
266 was unfavorable. The mesoscale dynamics of the Mistral wind over the Gulf of Lion was detailed in
267 *Drobinski et al. [2017]*. They related boundary layer balloons observations in the marine atmospheric
268 boundary layer with the AROME-WMED weather forecast model and analyzed all the terms of the
269 Lagrangian formulation of the momentum conservation equation to identify forces acting in the
270 injection, ejection and deceleration regions of the Mistral flow.

271 Several articles have addressed the determination of air/sea fluxes at different spatial and
272 temporal scales. Airborne measurements enabled to characterize the mean and turbulent structure
273 of the marine atmospheric boundary layer [*Brilouet et al., 2017*]. They showed that a one-
274 dimensional description of the vertical exchanges remains problematic because of the presence in
275 the marine atmospheric boundary layer of organized structures such as two-dimensional rolls
276 favored by strong winds and surface heat fluxes. *Caniaux et al. [2017]* using measurements at the air
277 sea interface and in the water column implemented an inverse method to estimate heat and water
278 fluxes during one year for the NWM basin at a fine scale resolution. They compared air-sea fluxes
279 adjusted using observations, with some operational numerical weather prediction models (such as
280 ARPEGE, NCEP, ERA-INTERIM, ECMWF, and AROME) and concluded that these models were unable
281 to retrieve the mean annual patterns and values of fluxes. *Song and Yu [2017]* performed an analysis

282 of the whole Mediterranean Sea surface energy budget using nine surface heat flux climatologies
283 obtained from atmospheric re-analyses, satellite or ship observations. They compared them with the
284 heat flux associated to the net transport through the Strait of Gibraltar and to data-assimilated global
285 ocean state estimation.

286 Uncertainties on heat and water fluxes, in particular related to uncertainties in the
287 parameterization of turbulent fluxes under strong wind conditions, remain an important problem for
288 ocean modeling in the Mediterranean, as shown by the sensitivity study by *Seyfried et al.* [2017] on
289 the modeling of the convection during winter 2012-2013. Unfortunately, no direct observation of the
290 turbulent fluxes was available during the strong wind events of DeWEX/ HyMeX SOP2. However, it
291 can be noted that the uncertainties of turbulent fluxes parameterization are not specific to the
292 Mediterranean.

293

294 **3.2. Interannual variability of dense water formation**

295 The currently well-accepted hypothesis based on the climate projections, predicts a strong
296 decrease of DWF rate, as surface layers will become too warm to produce dense waters. On the
297 other hand, increasing evaporation should increase the surface water salinity, which could, in turn,
298 raise density and result in convection. So, at least cyclically the Mediterranean should continue to
299 produce dense water through different mechanisms; however, under this scenario, deep water
300 characteristics should be deeply modified, affecting nutrient budgets and the whole ecosystem
301 functioning.

302 The interannual variability of convection in the Gulf of Lion over the last few decades has not
303 been monitored consistently and uniformly; CTD profiles and short-term mooring lines have been
304 used to document the period from 1970 to 2000 [see *Béthoux et al.*, 2002; *Mertens and Schott*,
305 1998]. It is only since 2007, with the implementation and simultaneous use, in the framework of
306 MOOSE in particular, of fully instrumented mooring lines and buoy at the Lion site, satellite data,
307 gliders, profiling floats and annual cruises throughout the NWM that a reference dataset has been
308 established to characterize the DWF interannual variability in terms of mixed layer depth, convective
309 surface, DWF rate or water mass characteristics, which allowed to evaluate accurately long-term
310 model simulations.

311 High frequency temperature, salinity and current measurements, collected at the Lion site
312 [*Durrieu de Madron et al.*, 2017; *Houpert et al.*, 2016], revealed that from 2007 to 2015 bottom
313 reaching convection and production of new WMDW, denser than 29.11 kg.m^{-3} , occurred every
314 winter between 2009 and 2013. The overlapping of the mixing and restratification phases was

315 regularly observed, with a secondary vertical mixing event of 2-4 days long occurring after the
316 beginning of the restratification phase (generally in April). This pattern is retrieved in the simulations
317 produced by [Léger *et al.*, 2016] or *in situ data* detailed by [Severin *et al.*, 2014; Severin *et al.*, 2016].

318 As expected, the succession of bottom-reaching convection episodes between 2009 and 2013
319 altered the deep-water masses thermohaline characteristics, which already underwent a significant
320 change after exceptional winter 2005 convection event [see Herrmann *et al.*, 2010 and references
321 therein]. The stepwise rise in temperature, salinity and density, observed consecutively to each
322 bottom-reaching convection event, led between 2009 to 2013 to an increasing trend in salinity ($+3.3$
323 $\pm 0.2 \cdot 10^{-3} \text{ a}^{-1}$) and potential temperature ($+3.2 \pm 0.5 \cdot 10^{-3} \text{ }^\circ\text{C}\cdot\text{a}^{-1}$) for the deep layer [Houpert *et al.*,
324 2016]. This confirmed the increase in rate observed from literature ($+9.2 \cdot 10^{-4} \text{ a}^{-1}$ in salinity and $+2 \cdot 10^{-3}$
325 $^\circ\text{C a}^{-1}$ in temperature for 1945-2000 period [Vargas-Yáñez *et al.*, 2010]. These increasing trends in
326 the deep layers would result from a heat and salt accumulation during the 1990s in the surface and
327 intermediate layers of the Gulf of Lion, transferred stepwise towards the deep layers when intense
328 convective events occur [like in 1999, 2005 and later; Somot *et al.*, 2016].

329 The evolution of the deep water thermohaline characteristics due to winter convection
330 depends directly on the volume of newly formed dense water. However, to get such estimates
331 remains a complex issue since there is currently no objective criterion for assessing them. Two
332 different methods were primarily used to estimate the volume of new WMDW, the advantages and
333 disadvantages of each are explained by Testor *et al.* [2018]. First, as the vertical dilution effect of
334 convection reduces the chlorophyll concentration [Severin *et al.*, 2014], the volume of new WMDW
335 can be approximated as the extent of the chlorophyll depleted mixing zone seen by ocean color
336 satellite times the mixed layer depth. Second, the volume of new WMDW can be estimated by
337 quantifying the amount of new water exceeding a given density threshold (e.g. $> 29.11 \text{ kg}\cdot\text{m}^{-3}$, the
338 maximum density of the "old" deep water) over the NWM basin. Houpert *et al.* [2016] estimated that
339 between 2009 and 2012, the new WMDW formation rate varied between 0.91 and 1.25 Sv (when
340 averaged over one year). As for them, Herrmann *et al.* [2017] used altimetry and ocean color
341 satellites data to obtain a wider annual volume range of 0.0 to 2.67 Sv for the 1998-2016 period.

342

343 **3.3. Deep water formation during winter 2013**

344 The winter buoyancy fluxes in 2012-2013 were sufficient to trigger deep convection and
345 significant production of new WMDW during DeWEX operations. With an observing system
346 simulation experiment approach, Waldman *et al.* [2016] confirmed the ability of the observation
347 network (ship track in Fig.2) to correctly quantify the spatial extent of convection and the seasonal

348 evolution of dense water volume. Several estimations of DWF rate deduced from observations of the
349 mixed patch volume [Herrmann et al., 2017], dissolved oxygen ventilation of the deep waters
350 [Coppola et al., 2017], and the newly formed dense water volume [Herrmann et al., 2017; Testor et
351 al., 2018] were coherent and ranged between 1.27 and 2.0 Sv. This last method, which appears to be
352 the most robust, was used to quantify the rate of dense water formation for the different models
353 used.

354 All the observations provided important results for model evaluation and sensitivity studies.
355 Numerical models were generally able to simulate realistic DWF (location, triggering and chronology,
356 characteristics) during winter 2013 [Estournel et al., 2016a; Lebeaupin Brossier et al., 2017; Léger et
357 al., 2016; Waldman et al., 2017a; Waldman et al., 2017b], and calculated DWF rates between 1.33
358 and 2.59 Sv.

359 Sensitivity analysis revealed that models are mostly affected by fine-scale ocean structures,
360 such as shelf DWF and export, eddies and fronts at the rim of the convective patch well evidenced by
361 glider observations [Testor et al., 2018]. The resolution of the mesoscale definitively improved the
362 realism of the simulations and their agreement with observations, by increasing the eddy kinetic
363 energy and enhancing the stratifying effect of advection through the mixed patch [Estournel et al.,
364 2016a; Lebeaupin Brossier et al., 2017; Waldman et al., 2017b]. Models also showed a large
365 sensitivity to the initial and boundary conditions (introducing bias on the stratification), the wind
366 intensity, and air-sea fluxes [Estournel et al., 2016a; Léger et al., 2016], which affect the water
367 masses characteristics and the volume of dense water formed during convection.

368

369 **3.4. Effects of small scales and intrinsic ocean variability on dense water formation**

370 The distinction between the internal (intrinsic) and external (atmospherically-forced)
371 components of the ocean variability is central to understand the forcings modulating DWF intensity
372 and water mass transformations. The large presence of meso- and sub-meso scale eddies, and
373 current instabilities in the NWM basin are sources of ocean intrinsic variability that can retroact on
374 the basin-scale circulation through an inverse energy cascade. The multiple platforms used during
375 the experience allowed identifying new dynamical processes at small scales or better characterizing
376 already known processes (frontal instabilities, convective plumes, vortices). Indeed, Giordani et al.
377 [2017] described a symmetric instability at the western edge of the deep convection area when
378 current and dominant northerly wind are in the same direction. This instability results from a cross-
379 front ageostrophic circulation, which subducts surface low-potential vorticity waters on the dense

380 side of the front and obducts high-potential vorticity waters from the pycnocline on the light side of
381 the front.

382 In the convection area, *Margirier et al. [2017]* were able from glider navigation data to
383 describe the statistical physical and biogeochemical characteristics of the convective plumes. It
384 appears that these plumes, which had radius of about 350 m and significant vertical velocities (up to
385 18 cm.s^{-1}), covered about one-third of the deep convection area. Vertical velocities are scaled by
386 atmospheric fluxes inducing downward buoyancy fluxes with a vertical diffusion coefficient of $7 \text{ m}^2.\text{s}^{-1}$.
387 *Bosse et al. [2016]* provided an inventory of the different types of cyclonic and anticyclonic
388 Submesoscale Coherent Vortices (SCVs) observed in the NWM by gliders, cruises, and mooring data
389 during a four-year period (2009-2013). They showed that these energetic features prevailed over the
390 large-scale geostrophic circulation and remained coherent for long periods of time (typically one
391 year). Bottom-reaching convection might favor the formation of cyclonic vortices. Using a realistic
392 high-resolution (1 km) numerical model, *Damien et al. [2017]* simulated the formation and spreading
393 of SCVs during intermediate and deep convection events. They reproduced similar long-lived cyclonic
394 and anticyclonic coherent structures. Both studies showed the prominent role of SCVs in the
395 spreading of the convected waters, their contribution to the ventilation of the deep basin, and their
396 influence on the convection onset the following winter.

397 *Estournel et al. [2016a]* discussed the interaction in autumn of the surface and Ekman
398 buoyancy fluxes associated with displacements of the front bounding the convection zone to the
399 south. They show that these processes are important for the convection preconditioning processes.
400 *Waldman et al. [2017a]* showed that intrinsic variability has a strong impact on the timing and
401 geographical extent of a convective event, but has little impact on the rate of convection in the
402 constrained 2012-2013 case. *Waldman et al. [2018]* further showed that intrinsic variability also
403 explains a significant fraction of the deep convection interannual variability, although it has only
404 modest impacts on the long-term mean state.

405

406 **3.5. Effect of dense water formation on biogeochemical budgets and primary production**

407 The DWF in the NWM impacts the nutrients distribution, matter export and development of the
408 trophic network and it strongly contributes to the modification of the deep stocks of these
409 components at the basin level. Three different areas of the western basin were identified by
410 contrasting vertical mixing regimes: deep convection, shallow convection and stratified area
411 [*Kessouri et al., 2018*]. Using a 3-D high-resolution coupled hydrodynamic-biogeochemical model
412 these authors showed in all three regions, that the mixed layer deepening during the destratification

413 process induced an upward nutrients flux, triggering in turn, an autumnal phytoplankton bloom. In
414 contrast at the end of winter, the end of turbulent mixing favored the onset of an intense spring
415 bloom only in the deep convection region. The authors concluded that despite these seasonal
416 variations, annual primary production in all three regions is quite similar, but total organic carbon
417 exported to deep waters was 3 and 8 times higher for moderate and deep convective areas
418 respectively, compared to stratified ones.

419 The depth reached by the convection directly drives the nutrient stoichiometry of water
420 masses in winter [Severin *et al.*, 2014; Severin *et al.*, 2017], which influences the phytoplankton
421 community structure in spring [Mayot *et al.*, 2017b; Severin *et al.*, 2016], which in return controls the
422 nutrient availability for the rest of the year by direct uptake [Kessouri *et al.*, 2017]. The general
423 emerging pattern is that the spatial (horizontal) extension of the convective area in winter influences
424 the intensity of the resulting bloom in spring (because of variable amount of nutrients injected into
425 the surface layer), but the depth (vertical) reached by the convection (and in particular when deep
426 convection reaches the nepheloid boundary layer) plays a key role in the bloom diversity (notably
427 due to different nutritional stoichiometry and higher Si:NO₃ ratio when convection is deeper)
428 [Leblanc *et al.*, 2018; Mayot *et al.*, 2017b]. These variations could be partly the result of pore water
429 release loaded with nutrients because of sediment resuspension enhanced by the bottom-reaching
430 mixing [Durrieu de Madron *et al.*, 2017].

431 Moreover, the deep convection events result in a homogenization of hydrological
432 characteristics, but also of the prokaryotic communities over the entire convective cell, resulting in a
433 surprising predominance of typical surface bacteria (such as *Oceanospirillales* and *Flavobacteriales*)
434 [Severin *et al.*, 2016]. However, physical turbulences only were not sufficient to explain this new
435 distribution, but act in synergy with quantity and quality of exported organic matter. Indeed, the
436 authors explained this dominance by the rapid export of fresh and labile organic matter to the deep
437 layers. Finally, the rapid return of specific prokaryotic communities and classic activities in the
438 intermediate layer less than 5 days after the intense mixing (and before hydrological restratification)
439 indicates a marked resilience of the communities, apart from the residual deep mixed water patch
440 [Severin *et al.*, 2017; Severin *et al.*, 2016]. Finally, the heterogeneous surface distribution of nutrients
441 during the winter deep convection event in the NWM was shown to impact the phytoplankton
442 distribution and community structure several weeks after the end of convective events [Mayot *et al.*,
443 2017b; Severin *et al.*, 2017; Severin *et al.*, 2016].

444 The multiple platforms of physical, bio-optical and biochemical measurements provided a
445 detailed characterization of the spatial and temporal structuring of the main biogeochemical
446 variables at different scales, from small-scale vortex structures to the basin as a whole. The role of

447 the post convective SCVs on nutrients distribution and phytoplankton communities, as well as on the
448 subsequent enhanced primary production and higher carbon sequestration was revealed by *Bosse et*
449 *al. [2017]*. They showed that SCVs present important dynamical barriers that drastically reduce
450 lateral exchanges between their cores and the surroundings thus enabling them to keep their core
451 characteristics the same for a long time. This suggests that they locally have a great imprint on both
452 physical and biogeochemical cycles. At larger scale, two distinct trophic regimes as “High Bloom”
453 centered on the convection area, and a “Bloom” bioregion located at its periphery were identified
454 [*Mayot et al., 2017a; Mayot et al., 2017b*], in agreement with regions mentioned above and defined
455 by *Kessouri et al. [2018]*.

456 The interannual variability of the physical and biogeochemical coupling of the NWM was also
457 assessed using satellite ocean color observations [*Mayot et al., 2017b*] and a 3-D hydrodynamic-
458 biogeochemical coupled model [*Ulses et al., 2016*]. Both studies showed that phytoplankton biomass
459 during the spring bloom is larger in years associated with intense deep convection events. Modeling
460 gave further evidence that amounts of nutrients annually injected into the surface layer is clearly
461 linked to the intensity of the convection but does not significantly modify the overall primary
462 production budget. Indeed, the primary production is inhibited during severe winters and transiently
463 explodes during the restratification phase, while it increases continuously during both phases when
464 winters are milder. As seen above, the occurrence of a highly productive bloom is also related to an
465 increase in the phytoplankton bloom size area. For the period including winter 2013, the processes
466 responsible for the stoichiometry variability at the seasonal scale were disentangled by using a
467 coupled physical-biogeochemical model able to correctly reproduce the general observed seasonal
468 dynamics of the physical and biogeochemical events [*Kessouri et al., 2017*]. The dynamics of the
469 nutrients, phyto- and zoo-plankton biomass as well as their interactions during the convection period
470 and the spring bloom were well reproduced. The authors estimated nutrient budgets for the entire
471 year and showed that the convection region represented a sink of inorganic and a source of organic
472 nitrogen and phosphorus. This process can efficiently export organic carbon below the photic layer
473 [*Kessouri et al., 2018; Kessouri et al., 2017; Severin et al., 2017*].

474

475 **3.6. Zooplankton community response to dense water formation**

476 The deep convection zone is likely an area of both enhanced energy transfer to higher trophic
477 levels and organic matter export [*Kessouri et al., 2018; Severin et al., 2017*]. The two trophic regimes
478 observed on the primary producer level are also reflected on higher trophic levels. Indeed in winter,
479 low zooplankton abundance and biomass were observed in the deep convection zone, but higher
480 values on its periphery. In spring, this pattern reversed with high biomass dominated by herbivorous

481 species in the deep convection zone, and lower values on the periphery [Donoso et al., 2017]. The
482 potential grazing impact of phytoplankton by zooplankton was estimated to increase by one order of
483 magnitude from winter to spring. In April, all areas except the deep convection zone incurred top-
484 down control by zooplankton [Siokou-Frangou et al., 2010].

485 Despite this significant seasonal variability of zooplankton biomass, the community composition
486 was comparable for both winter mixing and spring bloom periods, typified by high copepod
487 dominance [Donoso et al., 2017]. Using stable isotope mixing models, Hunt et al. [2017] estimated
488 that micro particulate organic matter never contributed more than 20% to zooplankton biomass,
489 even in regions where microphytoplankton was plentiful, indicating that a large part of its biomass
490 may have remained ungrazed.

491

492

493 **Acknowledgements**

494 Many people participated in this observational effort: scientists, technicians, crews.... All deserve our
495 grateful thanks. The main efforts were supported by CNRS, French universities (Sorbonne, Toulouse,
496 Marseille, Perpignan...), Météo-France, IFREMER, and CNES through the international
497 metaprogramme MISTRALS dedicated to the understanding of the Mediterranean basin
498 environmental processes (<http://www.mistrals-home.org>). More specifically by MERMEX-DEWEX,
499 MOOSE and HYMEX French programs.

500

501

502 **References**

- 503 Adloff, F., S. Somot, F. Sevault, G. Jordà, R. Aznar, M. Déqué, M. Herrmann, M. Marcos, C. Dubois, E.
504 Padorno, E. Alvarez-Fanjul, and D. Gomis, Mediterranean Sea response to climate change in
505 an ensemble of twenty first century scenarios, *Climate Dynamics*, 45 (9), 2775-2802, 2015.
- 506 Attané, I., and Y. Courbage, La démographie en Méditerranée. Situation et projections, in *Les*
507 *fascicules du Plan Bleu*, pp. 249, 2001.
- 508 Auger, P.A., C. Ulses, C. Estournel, L. Stemmann, S. Somot, and F. Diaz, Interannual control of
509 plankton communities by deep winter mixing and prey/predator interactions in the NW
510 Mediterranean: Results from a 30-year 3D modeling study, *Progress in Oceanography*, 124,
511 12-27, 2014.
- 512 Béthoux, J.-P., X. Durrieu de Madron, F. Nyffeler, and D. Tailliez, Deep water in the western
513 Mediterranean: peculiar 1999 and 2000 characteristics, shelf formation hypothesis,
514 variability since 1970 and geochemical inferences, *Journal of Marine Systems*, 33-34 (C), 117-
515 131, 2002.
- 516 Bosse, A., P. Testor, L. Houpert, P. Damien, L. Prieur, D. Hayes, V. Taillandier, X. Durrieu de Madron, F.
517 d'Ortenzio, L. Coppola, J. Karstensen, and L. Mortier, Scales and dynamics of Submesoscale

518 Coherent Vortices formed by deep convection in the northwestern Mediterranean Sea,
519 *Journal of Geophysical Research: Oceans*, 121 (10), 7716-7742, 2016.

520 Bosse, A., P. Testor, N. Mayot, L. Prieur, F. D'Ortenzio, L. Mortier, H.L. Goff, C. Gourcuff, L. Coppola,
521 H. Lavigne, and P. Raimbault, A submesoscale coherent vortex in the Ligurian Sea: From
522 dynamical barriers to biological implications, *Journal of Geophysical Research: Oceans*, 122
523 (8), 6196-6217, 2017.

524 Brilouet, P.-E., P. Durand, and G. Canut, The marine atmospheric boundary layer under strong wind
525 conditions: Organized turbulence structure and flux estimates by airborne measurements,
526 *Journal of Geophysical Research: Atmospheres*, 122 (4), 2016JD025960, 2017.

527 Cacho, I., J. Grimalt, and M. Canals, *Response of the Western Mediterranean Sea to rapid climatic*
528 *variability during the last 50,000 years: A molecular biomarker approach*, 253-272 pp., 2002.

529 Caniaux, G., L. Prieur, H. Giordani, and J.L. Redelsperger, An inverse method to derive surface fluxes
530 from the closure of oceanic heat and water budgets: Application to the north-western
531 Mediterranean Sea, *Journal of Geophysical Research: Oceans*, 122 (4), 2884-2908, 2017.

532 Conan, P., C.M. Turley, E. Stutt, M. Pujo-Pay, and F. Van Wambeke, Relationship between
533 Phytoplankton Efficiency and the Proportion of Bacterial Production to Primary Production in
534 the Mediterranean Sea, *Aquatic Microbial Ecology*, 17 (2), 131-144, 1999.

535 Coppola, L., L. Prieur, I. Taupier-Letage, C. Estournel, P. Testor, D. Lefevre, S. Belamari, S. LeReste,
536 and V. Taillandier, Observation of oxygen ventilation into deep waters through targeted
537 deployment of multiple Argo-O2 floats in the north-western Mediterranean Sea in 2013,
538 *Journal of Geophysical Research: Oceans*, 122 (8), 6325-6341, 2017.

539 Crise, A., J.I. Allen, J. Baretta, G. Crispi, R. Mosetti, and C. Solidoro, The Mediterranean pelagic
540 ecosystem response to physical forcing, *Progress In Oceanography*, 44 (1-3), 219-243, 1999.

541 D'Ortenzio, F., and M. Ribera d'Alcalà, On the trophic regimes of the Mediterranean Sea: a satellite
542 analysis, *Biogeosciences*, 6 (2), 139-148, 2009.

543 Damien, P., A. Bosse, P. Testor, P. Marsaleix, and C. Estournel, Modeling postconvective
544 submesoscale coherent vortices in the northwestern Mediterranean Sea, *Journal of*
545 *Geophysical Research: Oceans*, n/a-n/a, 2017.

546 Diaz, F., P. Raimbault, and P. Conan, Small-scale study of primary productivity during spring in a
547 Mediterranean coastal area (Gulf of Lions), *Continental Shelf Research*, 20 (9), 975-996, 2000.

548 Donoso, K., F. Carlotti, M. Pagano, B.P.V. Hunt, R. Escibano, and L. Berline, Zooplankton community
549 response to the winter 2013 deep convection process in the NW Mediterranean Sea, *Journal*
550 *of Geophysical Research: Oceans*, 122 (3), 2319-2338, 2017.

551 Drobinski, P., B. Alonzo, C. Basdevant, P. Cocquerez, A. Doerenbecher, N. Fourrié, and M. Nuret,
552 Lagrangian dynamics of the mistral during the HyMeX SOP2, *Journal of Geophysical Research:*
553 *Atmospheres*, 122 (3), 2016JD025530, 2017.

554 Durrieu de Madron, X., S. Ramondenc, L. Berline, L. Houpert, A. Bosse, S. Martini, L. Guidi, P. Conan,
555 C. Curtil, N. Delsaut, S. Kunesch, J.F. Ghiglione, P. Marsaleix, M. Pujo-Pay, T. Séverin, P.
556 Testor, C. Tamburini, and Antares collaboration, Deep sediment resuspension and thick
557 nepheloid layer generation by open-ocean convection, *Journal of Geophysical Research:*
558 *Oceans*, 122 (3), 2291-2318, 2017.

559 Estournel, C., P. Testor, P. Damien, F. D'Ortenzio, P. Marsaleix, P. Conan, F. Kessouri, X. Durrieu de
560 Madron, L. Coppola, J.-M. Lellouche, S. Belamari, L. Mortier, C. Ulses, M.-N. Bouin, and L.
561 Prieur, High resolution modeling of dense water formation in the north-western
562 Mediterranean during winter 2012–2013: Processes and budget, *Journal of Geophysical*
563 *Research: Oceans*, 121 (7), 5367-5392, 2016a.

564 Estournel, C., P. Testor, I. Taupier-Letage, M.-N. Bouin, L. Coppola, P. Durand, P. Conan, A. Bosse, P.-
565 E. Brilouet, L. Beguery, S. Belamari, K. Béranger, J. Beuvier, D. Bourras, G. Canut, A.
566 Doerenbecher, X. Durrieu de Madron, F. D'Ortenzio, P. Drobinski, V. Ducrocq, N. Fourrié, H.
567 Giordani, L. Houpert, L. Labatut, C.L. Brossier, M. Nuret, L. Prieur, O. Roussot, L. Seyfried, and
568 S. Somot, HyMeX-SOP2: The Field Campaign Dedicated to Dense Water Formation in the
569 Northwestern Mediterranean, *Oceanography*, 29 (4), 196-206, 2016b.

570 Giordani, H., C. Lebeaupin-Brossier, F. Léger, and G. Caniaux, A PV-approach for dense water
571 formation along fronts: Application to the Northwestern Mediterranean, *Journal of*
572 *Geophysical Research: Oceans*, 122 (2), 995-1015, 2017.

573 Giorgi, F., Climate change hot-spots, *Geophysical Research Letters*, 33 (8), 2006.

574 Grignon, L., D.A. Smeed, H.L. Bryden, and K. Schroeder, Importance of the Variability of Hydrographic
575 Preconditioning for Deep Convection in the Gulf of Lion, NW Mediterranean, *Ocean Science*,
576 6 (2), 573-586, 2010.

577 Herrmann, M., P.-A. Auger, C. Ulses, and C. Estournel, Long-term monitoring of ocean deep
578 convection using multisensors altimetry and ocean color satellite data, *Journal of Geophysical*
579 *Research: Oceans*, 122 (2), 1457-1475, 2017.

580 Herrmann, M.J., F. Sevault, J. Beuvier, and S. Somot, What induced the exceptional 2005 convection
581 event in the northwestern Mediterranean basin? Answers from a modeling study, *Journal of*
582 *Geophysical Research: Oceans*, 115 (C12), 2010.

583 Houpert, L., X. Durrieu de Madron, P. Testor, A. Bosse, F. D'Ortenzio, M.N. Bouin, D. Dausse, H. Le
584 Goff, S. Kunesch, M. Labaste, L. Coppola, L. Mortier, and P. Raimbault, Observations of open-
585 ocean deep convection in the northwestern Mediterranean Sea: Seasonal and interannual
586 variability of mixing and deep water masses for the 2007-2013 Period, *Journal of Geophysical*
587 *Research: Oceans*, 121 (11), 8139-8171, 2016.

588 Hunt, B.P.V., F. Carlotti, K. Donoso, M. Pagano, F. D'Ortenzio, V. Taillandier, and P. Conan, Trophic
589 pathways of phytoplankton size classes through the zooplankton food web over the spring
590 transition period in the north-west Mediterranean Sea, *Journal of Geophysical Research:*
591 *Oceans*, 122 (8), 6309-6324, 2017.

592 Kessouri, F., C. Ulses, C. Estournel, P. Marsaleix, F. D'Ortenzio, T. Severin, V. Taillandier, and P. Conan,
593 Vertical Mixing Effects on Phytoplankton Dynamics and Organic Carbon Export in the
594 Western Mediterranean Sea, *Journal of Geophysical Research: Oceans*, 0 (0), 2018.

595 Kessouri, F., C. Ulses, C. Estournel, P. Marsaleix, T. Severin, M. Pujo-Pay, J. Caparros, P. Raimbault,
596 O.P.d. Fommervault, F. D'Ortenzio, V. Taillandier, P. Testor, and P. Conan, Nitrogen and
597 phosphorus budgets in the Northwestern Mediterranean deep convection region, *Journal of*
598 *Geophysical Research: Oceans*, 122 (12), 9429-9454, 2017.

599 Lacombe, H., and C. Richez, The regime of the Strait of Gibraltar, in *Hydrodynamics of semi-enclosed*
600 *seas*, edited by J.C.J. Nihoul, pp. 13-73, Elsevier, New York, 1982.

601 Lebeaupin Brossier, C., F. Léger, H. Giordani, J. Beuvier, M.-N. Bouin, V. Ducrocq, and N. Fourrié,
602 Dense water formation in the north-western Mediterranean area during HyMeX-SOP2 in
603 1/36° ocean simulations: Ocean-atmosphere coupling impact, *Journal of Geophysical*
604 *Research: Oceans*, 122 (7), 5749-5773, 2017.

605 Leblanc, K., B. Quéguiner, F. Diaz, V. Cornet, M. Michel-Rodriguez, X. Durrieu de Madron, C. Bowler,
606 S. Malviya, M. Thyssen, G. Grégori, M. Rembauville, O. Grosso, J. Poulain, C. de Vargas, M.
607 Pujo-Pay, and P. Conan, Nanoplanktonic diatoms are globally overlooked but play a role in
608 spring blooms and carbon export, *Nature Communications*, 9 (1), 953, 2018.

609 Léger, F., C. Lebeaupin Brossier, H. Giordani, T. Arsouze, J. Beuvier, M.-N. Bouin, É. Bresson, V.
610 Ducrocq, N. Fourrié, and M. Nuret, Dense water formation in the north-western
611 Mediterranean area during HyMeX-SOP2 in 1/36° ocean simulations: Sensitivity to initial
612 conditions, *Journal of Geophysical Research: Oceans*, 121 (8), 5549-5569, 2016.

613 Madec, G., P. Delecluse, M. Crépon, and F. Lott, Large-Scale Preconditioning of Deep-Water
614 Formation in the Northwestern Mediterranean Sea, *Journal of Physical Oceanography*, 26 (8),
615 1393-1408, 1996.

616 Margirier, F., A. Bosse, P. Testor, B. L'Hévéder, L. Mortier, and D. Smeed, Characterization of
617 Convective Plumes Associated With Oceanic Deep Convection in the Northwestern
618 Mediterranean From High-Resolution In Situ Data Collected by Gliders, *Journal of*
619 *Geophysical Research: Oceans*, 122 (12), 9814-9826, 2017.

620 Marty, J.C., and J. Chiavérini, Hydrological changes in the Ligurian Sea (NW Mediterranean, DYFAMED
621 site) during 1995–2007 and biogeochemical consequences, *Biogeosciences*, 7 (7), 2117-2128,
622 2010.

623 Mayot, N., F. D'Ortenzio, M. Ribera d'Alcalà, H. Lavigne, and H. Claustre, Interannual variability of the
624 Mediterranean trophic regimes from ocean color satellites, *Biogeosciences*, 13 (6), 1901-
625 1917, 2016.

626 Mayot, N., F. D'Ortenzio, V. Taillandier, L. Prieur, O.P.d. Fommervault, H. Claustre, A. Bosse, P. Testor,
627 and P. Conan, Physical and Biogeochemical Controls of the Phytoplankton Blooms in North
628 Western Mediterranean Sea: A Multiplatform Approach Over a Complete Annual Cycle
629 (2012–2013 DEWEX Experiment), *Journal of Geophysical Research: Oceans*, 122 (12), 9999-
630 10019, 2017a.

631 Mayot, N., F. D'Ortenzio, J. Uitz, B. Gentili, J. Ras, V. Vellucci, M. Golbol, D. Antoine, and H. Claustre,
632 Influence of the Phytoplankton Community Structure on the Spring and Annual Primary
633 Production in the Northwestern Mediterranean Sea, *Journal of Geophysical Research:
634 Oceans*, 122 (12), 9918-9936, 2017b.

635 MEDOC group, Observation of formation of deep water in the Mediterranean Sea, 1969, *Nature*, 227,
636 1037-1040, 1970.

637 MERMEX group, Marine ecosystems' responses to climatic and anthropogenic forcings in the
638 Mediterranean, *Progress In Oceanography*, 91 (2), 97-166, 2011.

639 Mertens, C., and F. Schott, Interannual Variability of Deep-Water Formation in the Northwestern
640 Mediterranean, *Journal of Physical Oceanography*, 28 (7), 1410-1424, 1998.

641 Paluszkiwicz, T., Deep Convective Plumes in the Ocean, *Oceanography*, 7, 1994.

642 Pujo-Pay, M., and P. Conan, Seasonal variability and export of Dissolved Organic Nitrogen in the
643 North Western Mediterranean Sea, *Journal of Geophysical Research*, 108 (C6), 1901-1911,
644 2003.

645 Pujo-Pay, M., P. Conan, L. Oriol, V. Cornet-Barthaux, C. Falco, J.F. Ghiglione, C. Goyet, T. Moutin, and
646 L. Prieur, Integrated survey of elemental stoichiometry (C, N, P) from the Western to Eastern
647 Mediterranean Sea, *Biogeosciences*, 8 (4), 883-899, 2011.

648 Ribera d'Alcalà, M., G. Civitarese, F. Conversano, and R. Lavezza, Nutrient ratios and fluxes hint at
649 overlooked processes in the Mediterranean Sea, *Journal of Geophysical Research*, 108 (C9),
650 8106, 2003.

651 Robinson, A.R., G. Wayne, A. Theocharis, and A. Lascaratos, Mediterranean Sea circulation, in
652 *Encyclopedia of Ocean Sciences*, edited by J. Steele, K. Turekian, and S. Thorpe, Academic
653 Press, 2001.

654 Santinelli, C., L. Nannicini, and A. Seritti, DOC dynamics in the meso and bathypelagic layers of the
655 Mediterranean Sea, *Deep Sea Research Part II: Topical Studies in Oceanography*, 57 (16),
656 1446-1459, 2010.

657 Severin, T., P. Conan, X. Durrieu de Madron, L. Houpert, M.J. Oliver, L. Oriol, J. Caparros, J.F.
658 Ghiglione, and M. Pujo-Pay, Impact of open-ocean convection on nutrients, phytoplankton
659 biomass and activity, *Deep Sea Research Part I: Oceanographic Research Papers*, 94 (0), 62-
660 71, 2014.

661 Severin, T., F. Kessouri, M. Rembauville, E.D. Sánchez-Pérez, L. Oriol, J. Caparros, M. Pujo-Pay, J.-F.
662 Ghiglione, F. D'Ortenzio, V. Taillandier, N. Mayot, X. Durrieu De Madron, C. Ulses, C.
663 Estournel, and P. Conan, Open-ocean convection process: A driver of the winter nutrient
664 supply and the spring phytoplankton distribution in the Northwestern Mediterranean Sea,
665 *Journal of Geophysical Research: Oceans*, 122 (6), 4587-4601, 2017.

666 Severin, T., C. Sauret, M. Boutrif, T. Duhaut, F. Kessouri, L. Oriol, J. Caparros, M. Pujo-Pay, X.D. de
667 Madron, M. Garel, C. Tamburini, P. Conan, and J.F. Ghiglione, Impact of an intense water
668 column mixing (0-1500m) on prokaryotic diversity and activities during an open-ocean
669 convection event in the NW Mediterranean Sea, *Environ Microbiol*, 2016.

670 Seyfried, L., P. Marsaleix, E. Richard, and C. Estournel, Modelling deep-water formation in the north-
671 west Mediterranean Sea with a new air–sea coupled model: sensitivity to turbulent flux
672 parameterizations, *Ocean Sci.*, 13 (6), 1093-1112, 2017.

673 Siokou-Frangou, I., U. Christaki, M.G. Mazzocchi, M. Montresor, M. Ribera d'Alcalá, D. Vaqué, and A.
674 Zingone, Plankton in the open Mediterranean Sea: a review, *Biogeosciences*, 7 (5), 1543-
675 1586, 2010.

676 Somot, S., L. Houpert, F. Sevault, P. Testor, A. Bosse, I. Taupier-Letage, M.-N. Bouin, R. Waldman, C.
677 Cassou, E. Sanchez-Gomez, X. Durrieu de Madron, F. Adloff, P. Nabat, and M. Herrmann,
678 Characterizing, modelling and understanding the climate variability of the deep water
679 formation in the North-Western Mediterranean Sea, *Climate Dynamics*, 2016.

680 Somot, S., F. Sevault, and M. Déqué, Transient climate change scenario simulation of the
681 Mediterranean Sea for the twenty-first century using a high-resolution ocean circulation
682 model, *Climate Dynamics*, 27 (7), 851-879, 2006.

683 Song, X., and L. Yu, Air-sea heat flux climatologies in the Mediterranean Sea: Surface energy balance
684 and its consistency with ocean heat storage, *Journal of Geophysical Research: Oceans*, 122
685 (5), 4068-4087, 2017.

686 Stemmann, L., G. Gorsky, J.-C. Marty, M. Picheral, and J.-C. Miquel, Four-year study of large-particle
687 vertical distribution (0–1000m) in the NW Mediterranean in relation to hydrology,
688 phytoplankton, and vertical flux, *Deep Sea Research Part II: Topical Studies in Oceanography*,
689 49 (11), 2143-2162, 2002.

690 Testor, P., A. Bosse, L. Houpert, F. Margirier, L. Mortier, H. Legoff, D. Dausse, M. Labaste, J.
691 Karstensen, D. Hayes, A. Olita, A. Ribotti, K. Schroeder, J. Chiggiato, R. Onken, E. Heslop, B.
692 Mourre, F. D'ortenzio, N. Mayot, H. Lavigne, O.d. Fommervault, L. Coppola, L. Prieur, V.
693 Taillandier, X.D.d. Madron, F. Bourrin, G. Many, P. Damien, C. Estournel, P. Marsaleix, I.
694 Taupier-Letage, P. Raimbault, R. Waldman, M.N. Bouin, H. Giordani, G. Caniaux, S. Somot, V.
695 Ducrocq, and P. Conan, Multiscale Observations of Deep Convection in the Northwestern
696 Mediterranean Sea during Winter 2012–2013 Using Multiple Platforms, *Journal of*
697 *Geophysical Research: Oceans*, 123, 1745–1776, 2018.

698 Testor, P., and J.-C. Gascard, Large-Scale Spreading of Deep Waters in the Western Mediterranean
699 Sea by Submesoscale Coherent Eddies, *Journal of Physical Oceanography*, 33 (1), 75-87,
700 2003.

701 Ulises, C., P.A. Auger, K. Soetaert, P. Marsaleix, F. Diaz, L. Coppola, M.J. Herrmann, F. Kessouri, and C.
702 Estournel, Budget of organic carbon in the North-Western Mediterranean open sea over the
703 period 2004–2008 using 3-D coupled physical-biogeochemical modeling, *Journal of*
704 *Geophysical Research: Oceans*, 121 (9), 7026-7055, 2016.

705 Vandromme, P., L. Stemmann, L. Berline, S. Gasparini, L. Mousseau, F. Prejger, O. Passafiume, J.M.
706 Guarini, and G. Gorsky, Inter-annual fluctuations of zooplankton communities in the Bay of
707 Villefranche-sur-mer from 1995 to 2005 (Northern Ligurian Sea, France), *Biogeosciences*, 8
708 (11), 3143-3158, 2011.

709 Vargas-Yáñez, M., P. Zunino, A. Benali, M. Delpy, F. Pastre, F. Moya, M.d.C. García-Martínez, and E.
710 Tel, How much is the western Mediterranean really warming and salting?, *Journal of*
711 *Geophysical Research: Oceans*, 115 (C4), 2010.

712 Waldman, R., M. Herrmann, S. Somot, T. Arsouze, R. Benshila, A. Bosse, J. Chanut, H. Giordani, F.
713 Sevault, and P. Testor, Impact of the Mesoscale Dynamics on Ocean Deep Convection: The
714 2012–2013 Case Study in the Northwestern Mediterranean Sea, *Journal of Geophysical*
715 *Research: Oceans*, 122 (11), 8813-8840, 2017a.

716 Waldman, R., S. Somot, M. Herrmann, A. Bosse, G. Caniaux, C. Estournel, L. Houpert, L. Prieur, F.
717 Sevault, and P. Testor, Modeling the intense 2012–2013 dense water formation event in the
718 northwestern Mediterranean Sea: Evaluation with an ensemble simulation approach, *Journal*
719 *of Geophysical Research: Oceans*, 122 (2), 1297-1324, 2017b.

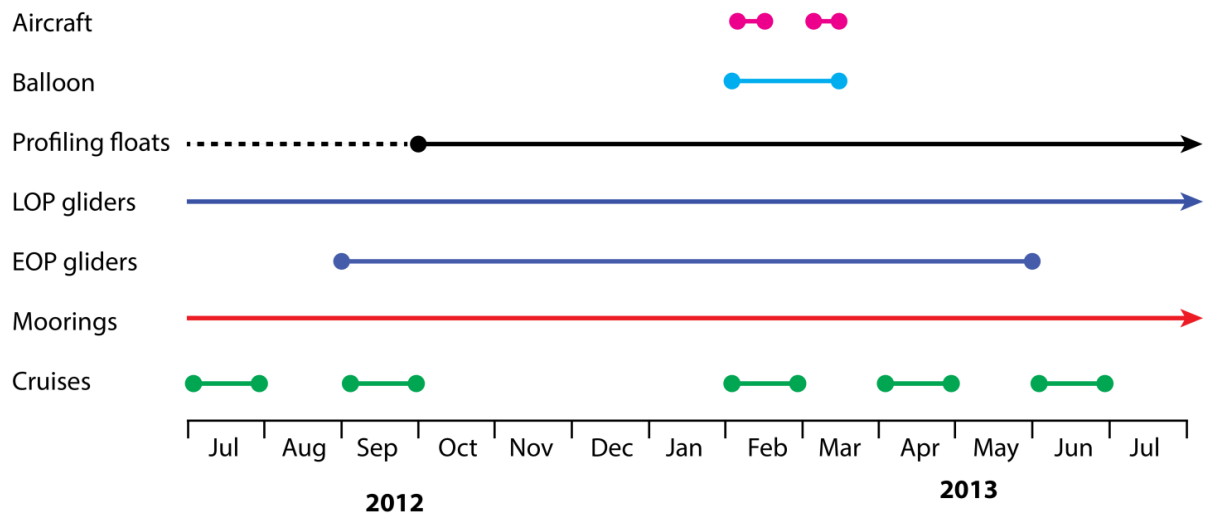
- 720 Waldman, R., S. Somot, M. Herrmann, F. Sevault, and P.E. Isachsen, On the Chaotic Variability of
721 Deep Convection in the Mediterranean Sea, *Geophysical Research Letters*, 45 (5), 2433-2443,
722 2018.
- 723 Waldman, R., S. Somot, M. Herrmann, P. Testor, C. Estournel, F. Sevault, L. Prieur, L. Mortier, L.
724 Coppola, V. Taillandier, P. Conan, and D. Dausse, Estimating dense water volume and its
725 evolution for the year 2012–2013 in the Northwestern Mediterranean Sea: An observing
726 system simulation experiment approach, *Journal of Geophysical Research: Oceans*, 121 (9),
727 6696-6716, 2016.
- 728

LEGENDS

Figure 1 - Time schedule of the different platforms and means used during the DEWEX experiment between July 2012 and July 2013

Figure 2 - Sketch of sampling strategy and examples of trajectory for airborne and oceanic platforms during the DEWEX experiment in the northwestern Mediterranean

Figure 3 - Side view of the airborne and oceanic platforms used during the DEWEX experiment



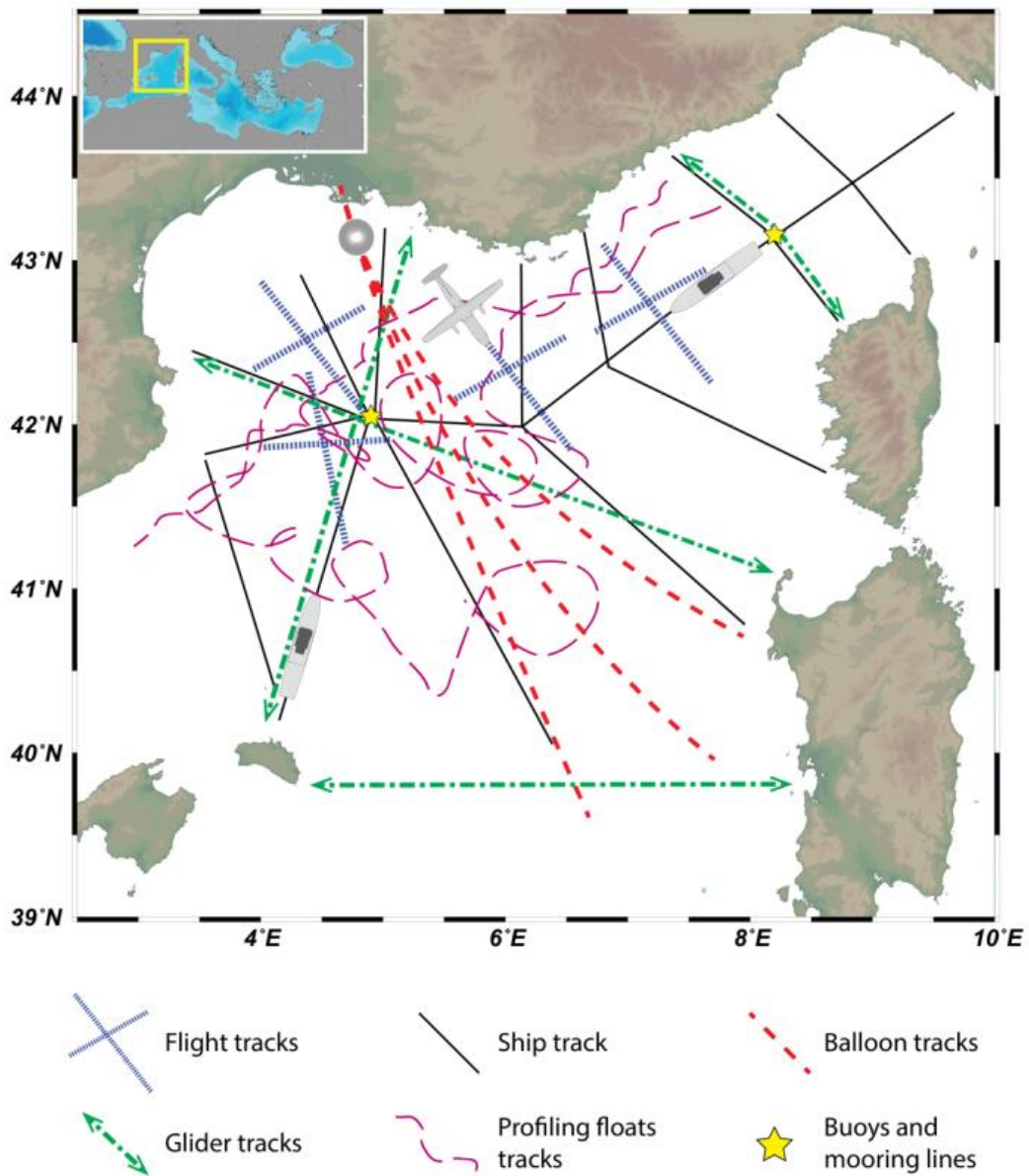
729

730 Figure 1 - Time schedule of the different platforms and means used during the DEWEX experiment
731 between July 2012 and July 2013

732

733

734



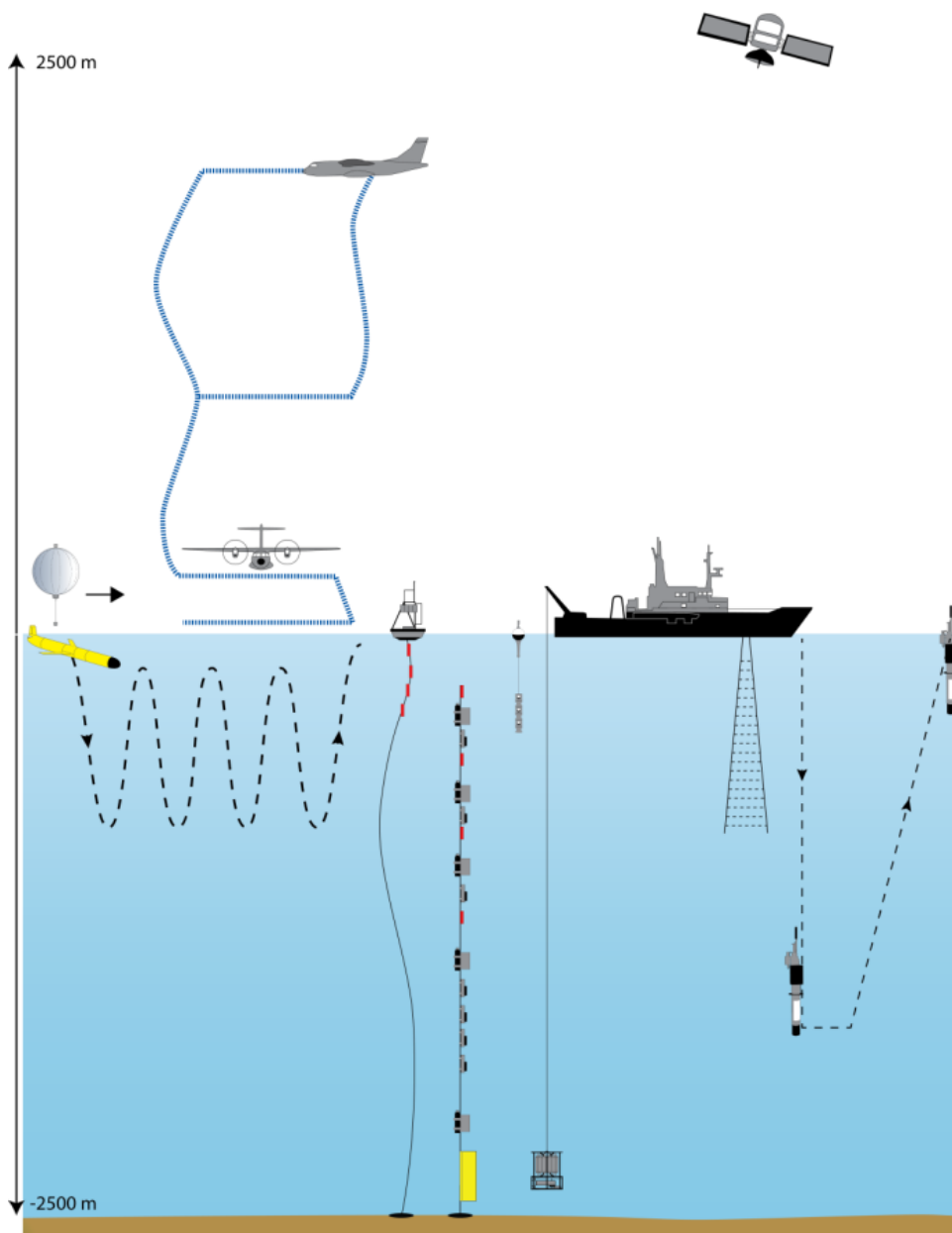
735

736

737 *Figure 2 - Sketch of sampling strategy and examples of trajectory for airborne and oceanic platforms*
738 *during the DEWEX experiment in the northwestern Mediterranean*

739

740



741

742

743 *Figure 3 - Side view of the airborne and oceanic platforms used during the DEWEX experiment*

744